Available online at www.sciencedirect.com
ScienceDirect
Powder Technology 182 (2008) 56–71
POWDER TECHNOLOGY
www.elsevier.com/locate/powtec

Drag on two coaxial rigid spheres moving along the axis of a cylinder filled with Carreau fluid

J.P. Hsu *, S.J. Yeh

Department of Chemical Engineering, National Taiwan University, Taipei, 10617 Taiwan

Received 29 January 2007; received in revised form 17 May 2007; accepted 21 May 2007
Available online 29 May 2007

Abstract

The boundary effect on the drag on two identical, rigid spheres moving along the axis of a long cylinder filled with a Carreau fluid for Reynolds number ranges from 0.1 to 40 is investigated. The influences of the key parameters of the problem under consideration, including the separation distance between two spheres, the relaxation time constant and the power-law index of a Carreau fluid, the Reynolds number, and the ratios (radius of sphere/radius of cylinder), on the drag acting on two spheres are investigated. We show that the boundary effect for the present case is more significant than that for the corresponding Newtonian fluid. The presence of the cylinder has the effect of enhancing the convective motion in the rear part of a sphere, thereby forming wakes and a reverse flow field, and this phenomenon is enhanced by the shear-thinning nature of a fluid. If the boundary effect is insignificant, the shear-thinning nature of a fluid has the effect of reducing the deviation of the ln(drag coefficient)-ln(Reynolds number) curve from a Stokes'-law-like relation. On the other hand, if it is significant, this deviation has a local minimum as the shear-thinning nature of a fluid varies.

Keywords: Sedimentation; Boundary effect; Drag coefficient; Two coaxial rigid spheres in cylinder; Carreau fluid

1. Introduction

Evaluating the drag on a particle as it translates through a fluid is a classic problem. Sedimentation, which is often used to estimate the physical properties of a particle, for instance, involves this problem. The fluidized bed often adopted in chemical plants is another typical example where the drag on a particle needs be evaluated. In practice, two important factors usually should be considered in the calculation of the drag on a particle, namely, the presence of a boundary such as container wall, and the influence of neighboring particles, especially when the concentration of particles is appreciable. In general, the former yields an extra retarding force on a moving particle, and the closer the particle to a boundary the slower its movement [1,2]. The latter depends largely on the concentration of particles, the relative orientation of neighboring particles, and the operating conditions such as Reynolds number.

The presence of a boundary and the neighboring particles on the drag on a particle has been investigated by many investigators. Stimson and Jeffery [3] presented a complete solution for the slow motion of two spheres parallel to their line of centers in an unbounded viscous fluid. Happel and Pfeffer [4] studied experimentally the falling of two spheres in a viscous liquid. Zhu et al. [5] developed a micro-force measuring system to directly measure the drag on two interacting particles at a medium large Reynolds number. Applying the same technique, Liang et al. [6] and Chen and Wu [7,8] measured the drag on two interacting rigid spheres in a Newtonian fluid. Greenstein [9] analyzed the drag on two spherical particles translating in a cylindrical tube filled with an incompressible viscous fluid. Maheshwari et al. [10] investigated the effect of blockage ratio (tube diameter/sphere diameter) on the steady flow and heat transfer characteristics of an incompressible Newtonian fluid over a sphere and an in-line array of three spheres placed at the axis of a tube.

* Corresponding author. Fax: +886 2 23623040.
E-mail address: jphsu@ntu.edu.tw (J.P. Hsu).

0032-5910/$ - see front matter © 2007 Elsevier B.V. All rights reserved.
doi:10.1016/j.powtec.2007.05.021

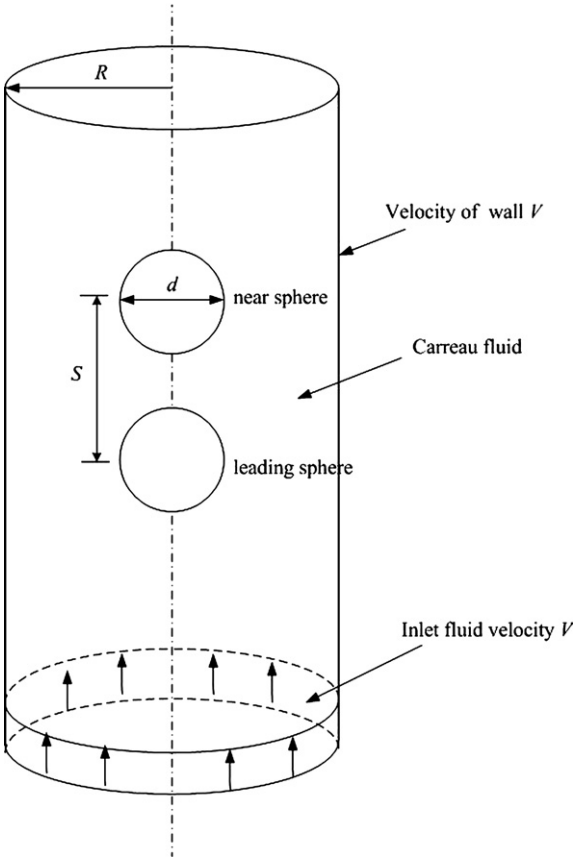

Fig. 1. Systematic representation of the problem considered where two identical, co-axial rigid spheres of diameter d move along the axis of a long cylinder of radius R filled with a Carreau fluid, S is the center-to-center distance between two spheres. For convenience, the spheres are fixed in space and both the bulk liquid and the cylinder wall move with a relative velocity V.

Many fluids encountered in industrial processes are of non-Newtonian nature where the rheological behavior of a fluid can differ appreciably from that of a Newtonian fluid [11–14]. In these cases, it is expected that the drag on a particle in the former can also be quite different from that in the latter. For instance, the drag on a particle in a shear-thinning fluid is expected to be smaller than that in the corresponding Newtonian fluid. Several attempts have been made recently regarding the behavior of a particle in a non-Newtonian fluid [15–20]. Missirlis et al. [21], for instance, studied the wall effect on the motion of a sphere in a shear-thinning power-law fluid at a low Reynolds number. Ceylan et al. [22] evaluated the drag on a rigid particle settling in a power-law fluid. Machač et al. [23,24] conducted the sedimentation of both spherical and non-spherical particles in a Carreau fluid in the creeping flow regime. Jaiswal et al. [25] modeled an unbounded slow flow of a power-law non-Newtonian fluid through an assemblage of spheres. Zhu et al. [26] investigated the drag on two interacting rigid spheres in a power-law pipe flow with a large (pipe diameter/sphere diameter) ratio. Hsu et al. [27] modeled theoretically the sedimentation of a spheroid in a cylindrical tube filled with a Carreau fluid for a low to medium value of Reynolds number. Daugan et al. [28,29] conducted an experimental study on the settling of two or three identical particles along their line of centres in a shear-thinning fluid at low Reynolds numbers. Maheshwari et al. [30] analyzed the hydrodynamic interaction between two rigid spheres tangentially translating in a power-law fluid.

The objective of this study is to analyze simultaneously the effects of particle–particle interaction, the presence of a boundary, and the non-Newtonian nature of a fluid on the drag on a particle. We consider the case of two identical, coaxial, rigid spheres moving along the axis of a long cylinder filled with a Carreau fluid. The influences of the separation distance between two spheres, the distance between spheres and cylinder wall, the Reynolds number, and the properties of a Carreau fluid, on the drag acting on the spheres are investigated.

2. Mathematical modeling

Referring to Fig. 1, we consider the moving of two identical, coaxial rigid spheres of diameter d along the axis of a long cylinder of radius R filled with a Carreau fluid. Let S be the

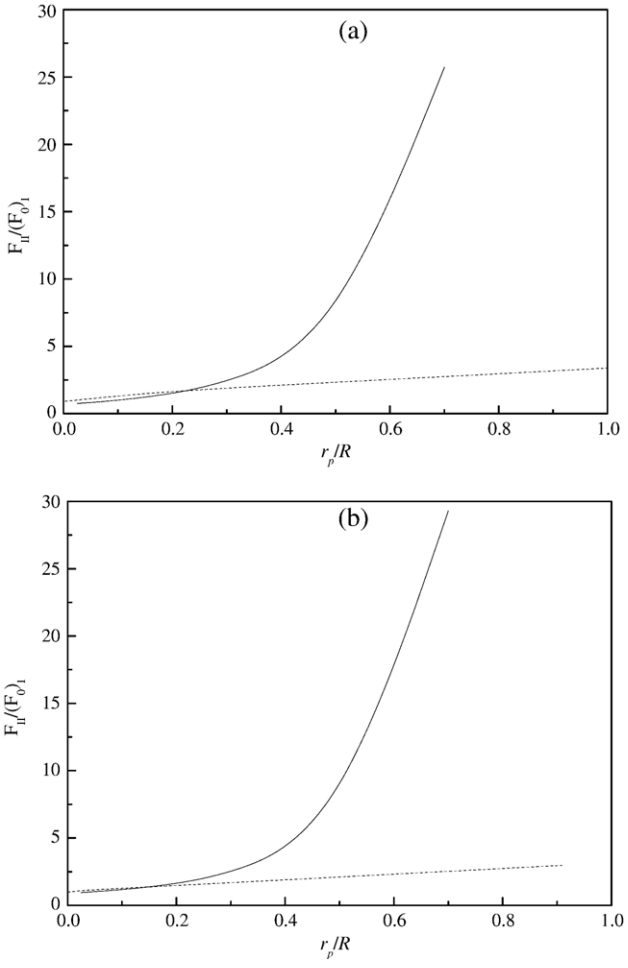

Fig. 2. Variation of scaled drag on two co-axial rigid spheres as a function of (r_p/R) at two levels of (S/d) for the case of a Newtonian fluid. Dashed curves, result of Greenstein [9], solid curves, present result. (a) $S/d=2$, (b) $S/d=11$.

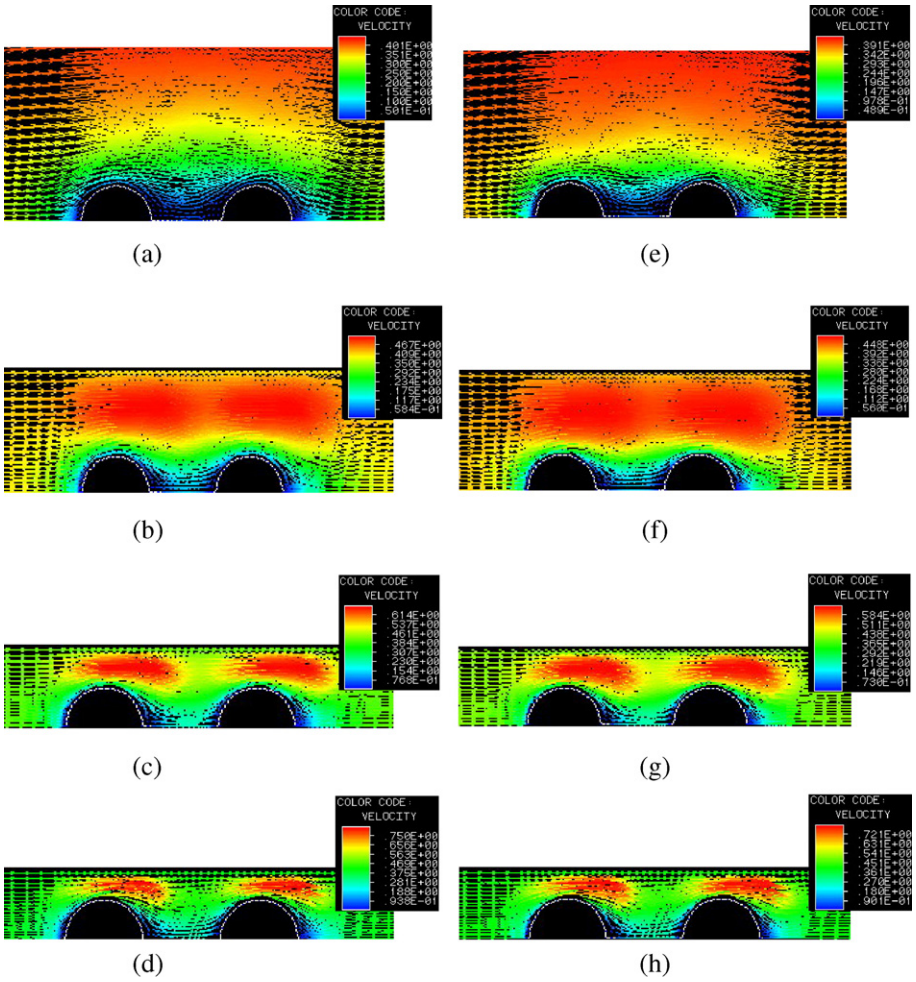

Fig. 3. Flow fields for various combinations of (r_p/R) and Cu at $S/d=2$ and $Re=0.1$. $Cu=0.1$ in (a), (b), (c), and (d), and $Cu=10$ in (e), (f), (g), and (h). (a) and (e), $r_p/R=0.1$, (b) and (f), $r_p/R=0.3$, (c) and (g), $r_p/R=0.5$, (d) and (h), $r_p/R=0.6$.

center-to-center distance between two spheres. For convenience, the spheres are held fixed and the bulk fluid moves with a relative velocity V.

Assuming incompressible fluid under steady-state condition, the flow field in the liquid phase can be described by

$$\rho \mathbf{u}\cdot\nabla\mathbf{u} = -\nabla P + \nabla\cdot\boldsymbol{\tau} \tag{1}$$

$$\nabla\cdot\mathbf{u} = 0 \tag{2}$$

In these expressions, ρ is the density of the fluid, P is the pressure, ∇ is the gradient operator, $\boldsymbol{\tau}$ is the stress tensor, and $\mathbf{u}$ is the fluid velocity. For a generalized Newtonian fluid, we have [14,31–33]

$$\boldsymbol{\tau} = -\eta(\dot{\gamma})\dot{\boldsymbol{\gamma}} \tag{3}$$

$$\dot{\boldsymbol{\gamma}} = (\nabla\mathbf{u} + (\nabla\mathbf{u})^{\mathrm{T}}) \tag{4}$$

where $\dot{\boldsymbol{\gamma}}$ is the rate-of-strain tensor, $\dot{\gamma}$ is the magnitude of the rate-of-strain tensor, η is the apparent viscosity, and the superscript T denotes matrix transpose. For the present Carreau fluid, we assume [14,31–33]

$$\eta(\dot{\gamma}) = \eta_\infty + (\eta_0 - \eta_\infty)[1 + (\lambda\dot{\gamma})^2]^{(n-1)/2} \tag{5}$$

where η_0 and η_∞ are respectively the viscosities corresponding to the minimum and the maximum shear rate, λ is the relaxation time constant, and n is the power-law index. For simplicity, η_∞ is neglected in subsequent analysis.

The following boundary conditions are assumed for the flow field:

$$u_z = V \quad \text{at} \quad r = R \tag{6}$$

$$u_z = V \text{ as } z \to \infty \tag{7}$$

$$u_z = 0 \quad \text{on sphere surface} \tag{8}$$

$$\frac{\partial \mathbf{u}}{\partial r} = 0, \; r = 0 \tag{9}$$

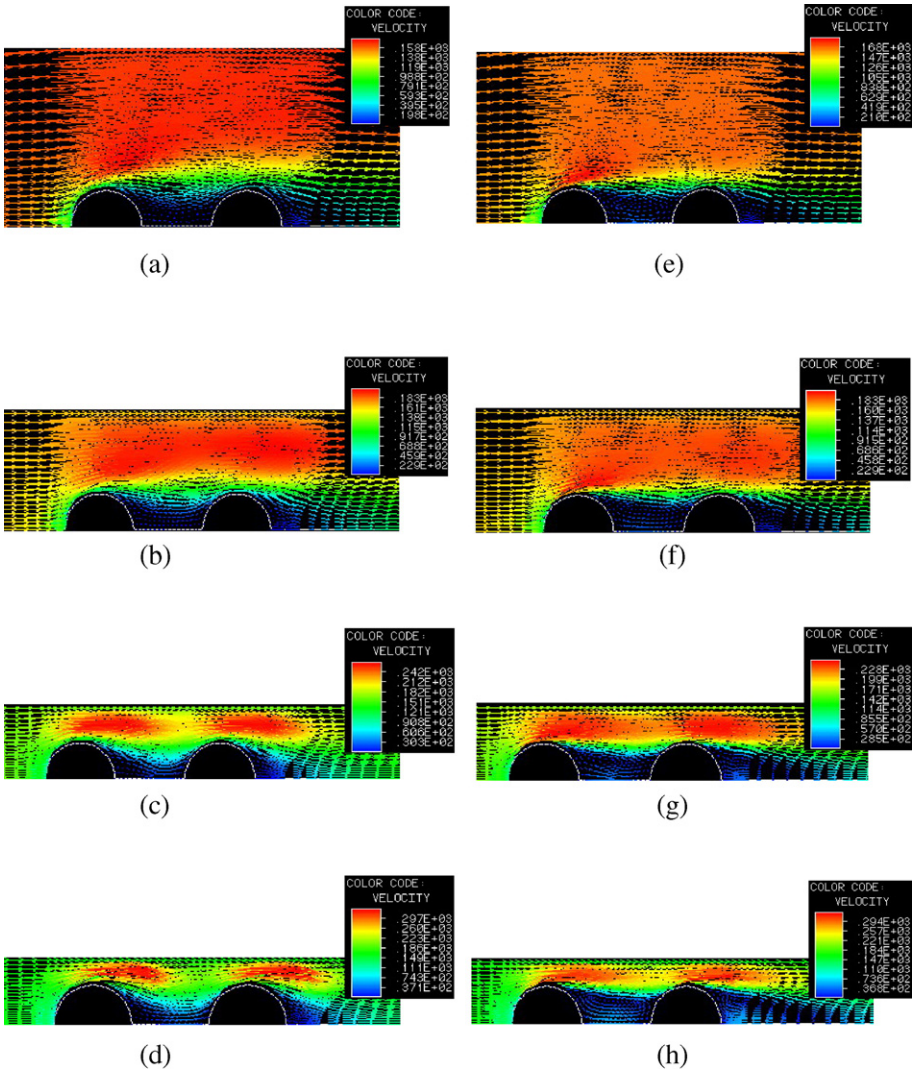

Fig. 4. Flow fields for various combinations of (r_p/R) and Cu at $S/d=2$ and $Re=40$. $Cu=0.1$ in (a), (b), (c), and (d), and $Cu=10$ in (e), (f), (g), and (h). (a) and (e), $r_p/R=0.1$, (b) and (f), $r_p/R=0.3$, (c) and (g), $r_p/R=0.5$, (d) and (h), $r_p/R=0.6$.

In these expressions, u_z is the fluid velocity in the z-direction. The last expression implies that the present problem is of symmetric nature, and solving the governing equations in half the tubular domain is sufficient.

The drag on a rigid sphere of radius r_p moving with a constant velocity V in an infinite, stagnant fluid of density ρ can be expressed as [14,34–36]

$$F = \left(\frac{1}{2}\rho V^2\right)(\pi r_p^2)C_D \tag{10}$$

where C_D is the drag coefficient. For Newtonian fluids, if V is in the creeping flow regime, C_D and the Reynolds number Re are related by the Stokes law [14,34,36,37],

$$C_D = \frac{24}{Re} \tag{11}$$

For the present case, a Stokes'-law-like relation can be expressed as

$$C_D = \frac{A(n, Cu, r_p/R)}{Re} \tag{12}$$

where $Cu=\lambda V/r_p$ is the Carreau number, and the Reynolds number is defined as $Re=2\rho r_p V/\eta_0$ [14,31–33]. Note tat if $Cu=0$, the fluid becomes Newtonian.

3. Results and discussion

FIDAP 7.6, a commercial software which is based on a Gelerkin finite element method with bilinear, four-node quadrilateral elements procedure, is chosen for the solution of the governing equations and the associated boundary conditions. Double precision is used throughout the computation, and grid independence is checked to ensure that the mesh used is

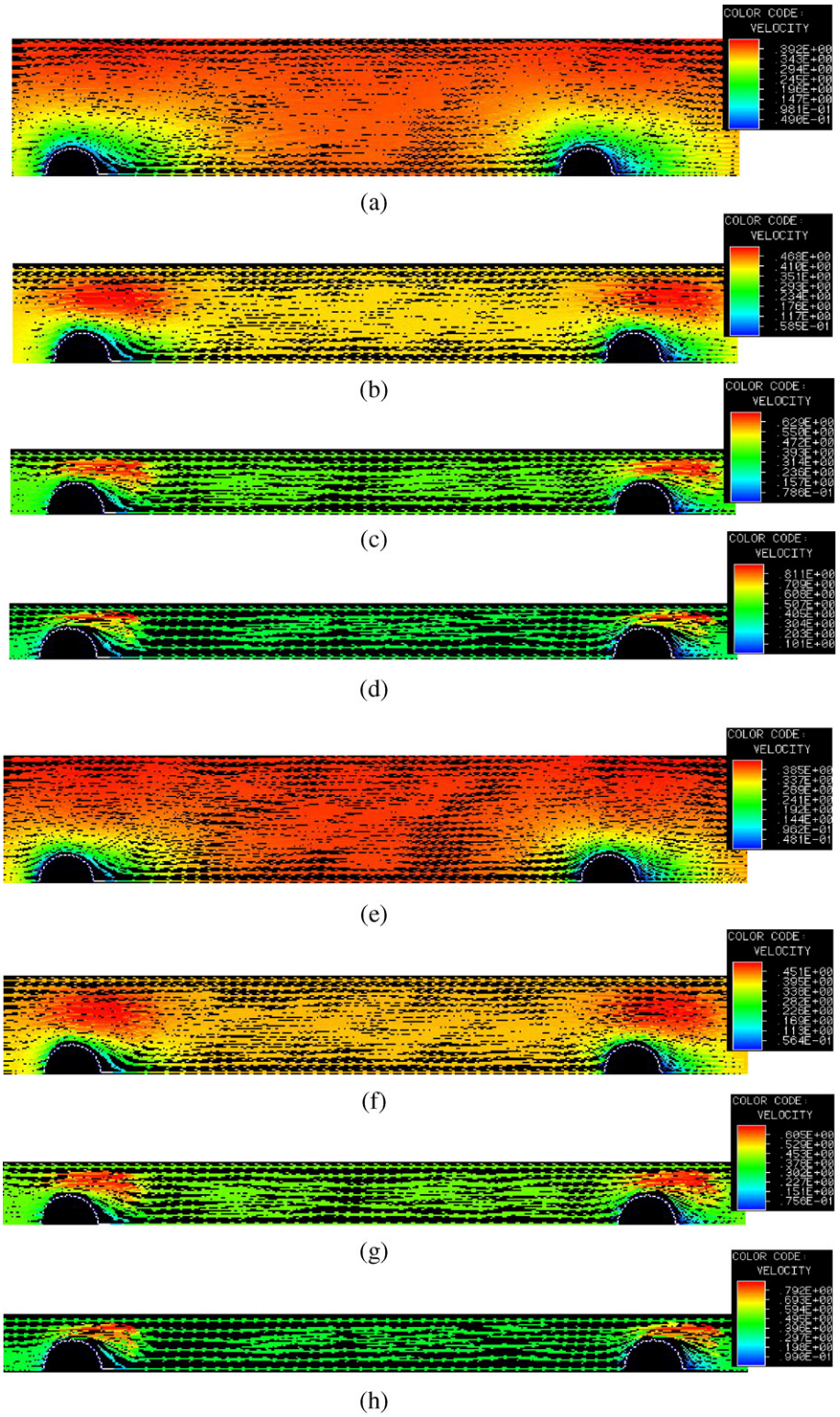

Fig. 5. Flow fields for various combinations of (r_p/R) and Cu at $S/d=10$ and $Re=0.1$. $Cu=0.1$ in (a), (b), (c), and (d), and $Cu=10$ in (e), (f), (g), and (h). (a) and (e), $r_p/R=0.1$, (b) and (f), $r_p/R=0.3$, (c) and (g), $r_p/R=0.5$, (d) and (h), $r_p/R=0.6$.

fine enough. A total of 18,706 elements are used in the fluid domain. The applicability of this software is justified by comparing the present result with that of Greenstein [9], which is based on a reflection method for the case of two spheres moving along the axis of a circular cylinder at a low *Re*. Fig. 2 shows the variations of $[F_{II}/(F_0)_I]$ as a function of (r_p/R) at two

levels of (S/d), $(F_0)_I$ and F_{II} are respectively the drag on a single sphere in an unbounded system and that on the rear sphere in a bounded system. Note that Greenstein's analysis is valid for weak wall and weak sphere–sphere interactions. Therefore, comparison between the present results and those of Greenstein's should be limited to small values of (r_p/R). In Fig. 2(b), $S/d=11$, the sphere–sphere interaction is unimportant and our results are very close to those predicted by Greenstein, implying that the performance of the software chosen is satisfactory.

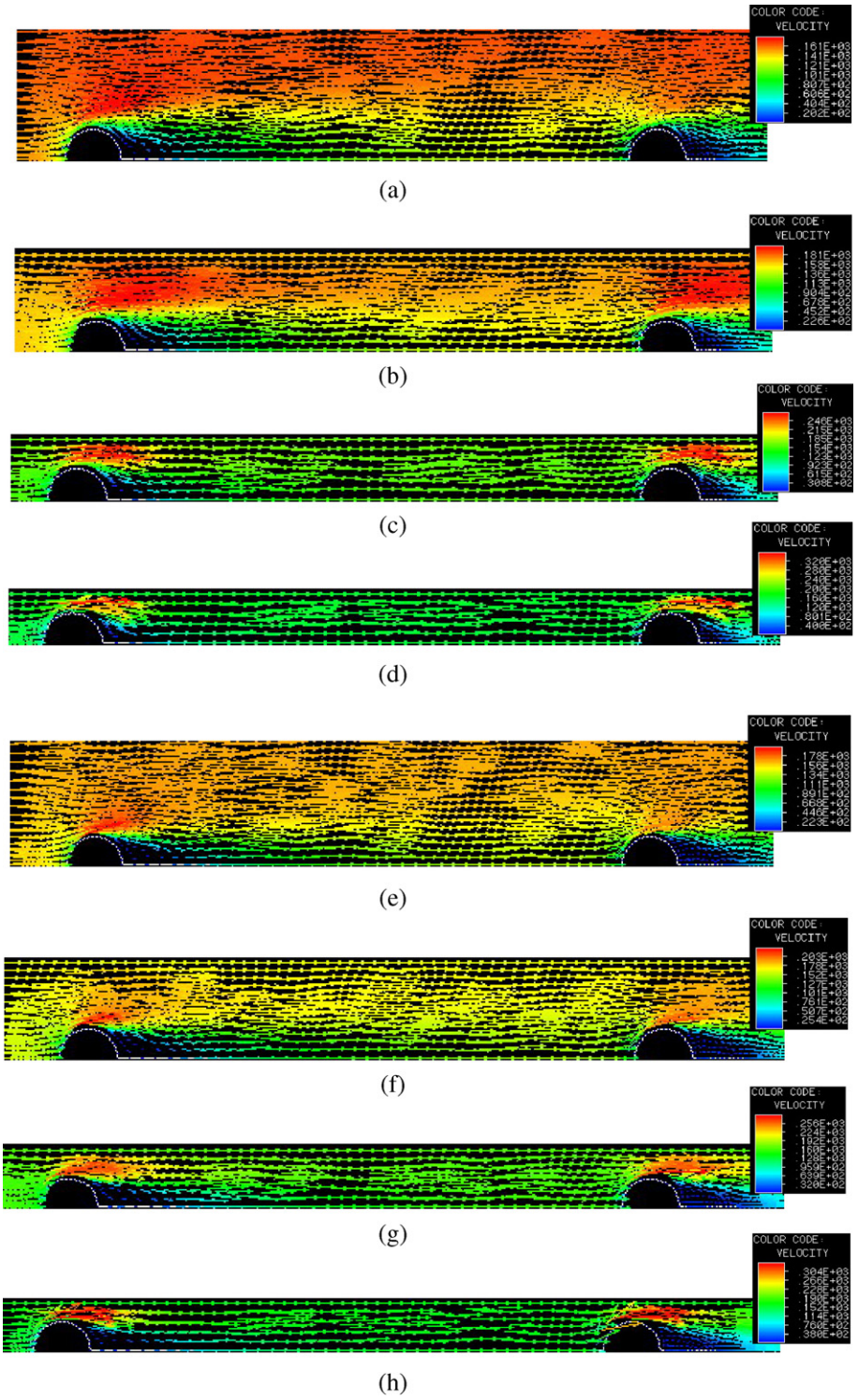

Fig. 6. Flow fields for various combinations of (r_p/R) and Cu at $S/d=10$ and $Re=40$. $Cu=0.1$ in (a), (b), (c), and (d), and $Cu=10$ in (e), (f), (g), and (h). (a) and (e), $r_p/R=0.1$, (b) and (f), $r_p/R=0.3$, (c) and (g), $r_p/R=0.5$, (d) and (h), $r_p/R=0.6$.

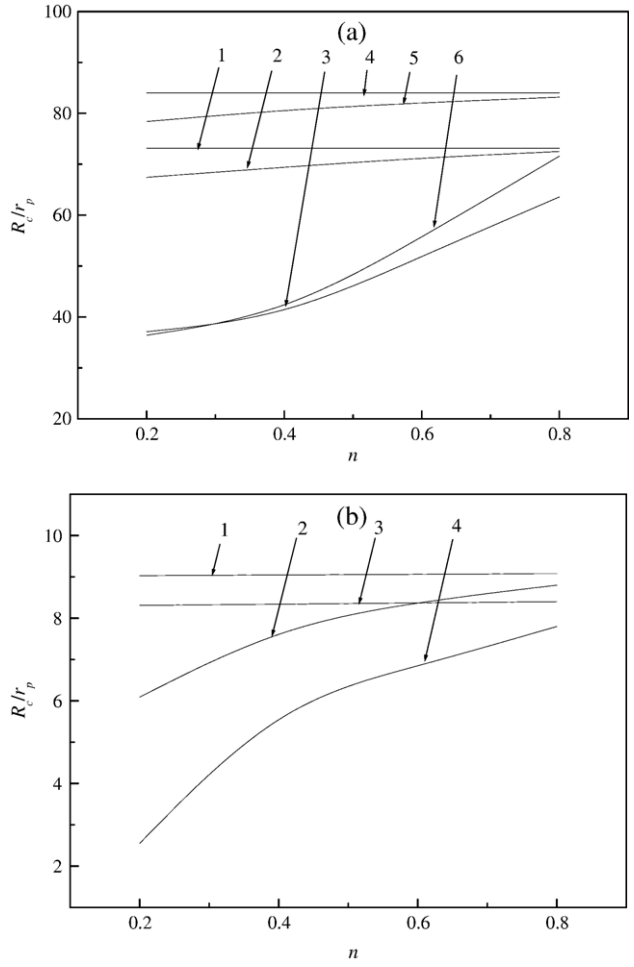

Fig. 7. Variations of (R_c/r_p) as a function of n for various combinations of (S/d), Cu, and Re. (a) $Re=0.1$. Curve 1, $S/d=2$ and $Cu=0.1$, 2, $S/d=2$ and $Cu=1$, 3, $S/d=2$ and $Cu=10$, 4, $S/d=10$ and $Cu=0.1$, 5, $S/d=10$ and $Cu=1$, 6, $S/d=10$ and $Cu=10$. (b) $Re=40$. Curve 1, $S/d=2$ and $Cu=0.1$, 2, $S/d=2$ and $Cu=1$, 3, $S/d=10$ and $Cu=0.1$, 4, $S/d=10$ and $Cu=1$.

3.1. Flow field

Fig. 3 shows the flow fields for various values of (r_p/R) at two levels of Cu for the case when $S/d=2$, $n=0.6$, and Re is relatively small; that for the case when Re is relatively large is presented in Fig. 4. Those for the case when $S/d=10$ are presented in Figs. 5 and 6. Figs. 3 and 5 reveal that if Re is small, regardless of the value of (S/d) the flow field in the front region of a sphere is symmetric to that in its rear region for the case when boundary effect is insignificant. In this case, the qualitatively nature of the flow field is uninfluenced by the presence of the boundary and the shear-thinning nature of a fluid. As shown in Figs. 4 and 6, the flow field becomes asymmetric when Re increases to 40. However, the presence of the cylinder wall has the effect of depressing the degree of asymmetry in the flow field, that is, the convective flow of fluid is confined by the cylinder wall. Fig. 4 shows that, due to the convective flow, boundary layer separation occurs in the rear region of a sphere and the direction of fluid flow is reversed. If the boundary effect is significant, the convective flow of a fluid is enhanced by its shear-thinning nature, so is the reverse in the direction of fluid flow. Therefore, if the boundary effect and/or the shear-thinning nature of a fluid are important, the reverse in the direction of fluid flow becomes appreciable, as shown in Fig. 4(h). The qualitative behaviors of the flow field shown in Fig. 6 are similar to that seen in Fig. 4. Fig. 5 suggests that if $Re=0.1$, the interaction between the flow field of the leading sphere and that of the rear sphere becomes unimportant when $S/d=10$. Although this interaction is appreciable when $Re=40$, as shown in Fig. 6, it is less significant than that for the case when $S/d=2$, and therefore, the reverse in the direction of fluid flow is not observed between two spheres.

3.2. Influence of boundary

The variations of the critical radius of a cylinder (R_c/r_p) as a function of n for various combinations of Cu and (S/d) at two levels of Re are illustrated in Fig. 7. The critical radius of a cylinder (R_c/r_p) is defined as the minimum (R/r_p) which yields $|\Delta(C_{D1}/\Delta(R/r_p)| \approx 5\%$. That is, if $(R/r_p)>(R_c/r_p)$, the boundary effect can be neglected. Fig. 7 shows that the smaller the Re the larger the (R_c/r_p). If both Cu and (S/d) are fixed, (R_c/r_p) declines with the decrease in n, regardless of the magnitude of Re. If $Re=0.1$, the smaller the (S/d) and/or the larger the Cu the smaller the (R_c/r_p) is. Fig. 7b suggests that if both Re and (S/d) are sufficiently large and the shear-thinning nature of a fluid is important (small n and/or large Cu), then (R_c/r_p) is small, implying that the boundary effect is unimportant. Zhu et al. [26] observed that the drag coefficient ratio of two interacting spheres in a power-law fluid with negligible boundary effect depends strongly on the separation distance between two spheres and the particle Reynolds number, but is independent of the power-law index. Fig. 7 indicates that if Cu is small (curves 1 and 4 of Fig. 7a, and curves 1 and 3 of Fig. 7b), (R_c/r_p) is insensitive to the variation of n, but sensitive to the variations of (S/d) and Re. This is consistent with the result of Zhu et al. [26]. Note that, however, if Cu becomes large (curves 3 and 6 of Fig. 7a, and curves 2 and 4 of Fig. 7b), (R_c/r_p) is sensitive to the variation of n.

The variations of the drag coefficient of the leading sphere C_{Dl} and that of the rear sphere C_{Dr} as a function of (r_p/R) at various combinations of Carreau numbers Cu and Re are illustrated in Fig. 8 for the case when $S/d=2$ and $n=0.6$. If Re is small, the drag on the leading sphere should close to that on the rear sphere, as is justified in Fig. 8a and b. However, if Re is sufficiently large, wakes are formed in the rear region of the leading sphere and the drag on the rear sphere is smaller than that when the leading sphere is absent, as is seen in Fig. 8c and d. Here, the larger the (r_p/R) the more significant the boundary effect, therefore C_D increases with the increase in (r_p/R). For a fixed value of (r_p/R), C_D decreases with the increase in Cu because the larger the value of Cu the more important the effect of shear thinning. If $r_p/R=0$ and $Re=0.1$, $(C_{Dl}(Cu=1)=0.97C_{Dl}(Cu=0))$, $(C_{Dr}(Cu=1)=0.97C_{Dr}(Cu=0))$, $(C_{Dl}(Cu=10)=0.65C_{Dl}(Cu=0))$, and $(C_{Dr}(Cu=10)=0.66C_{Dr}(Cu=0))$; if $r_p/R=0$ and $Re=40$, $(C_{Dl}(Cu=1)=0.83C_{Dl}(Cu=0))$, $(C_{Dr}$

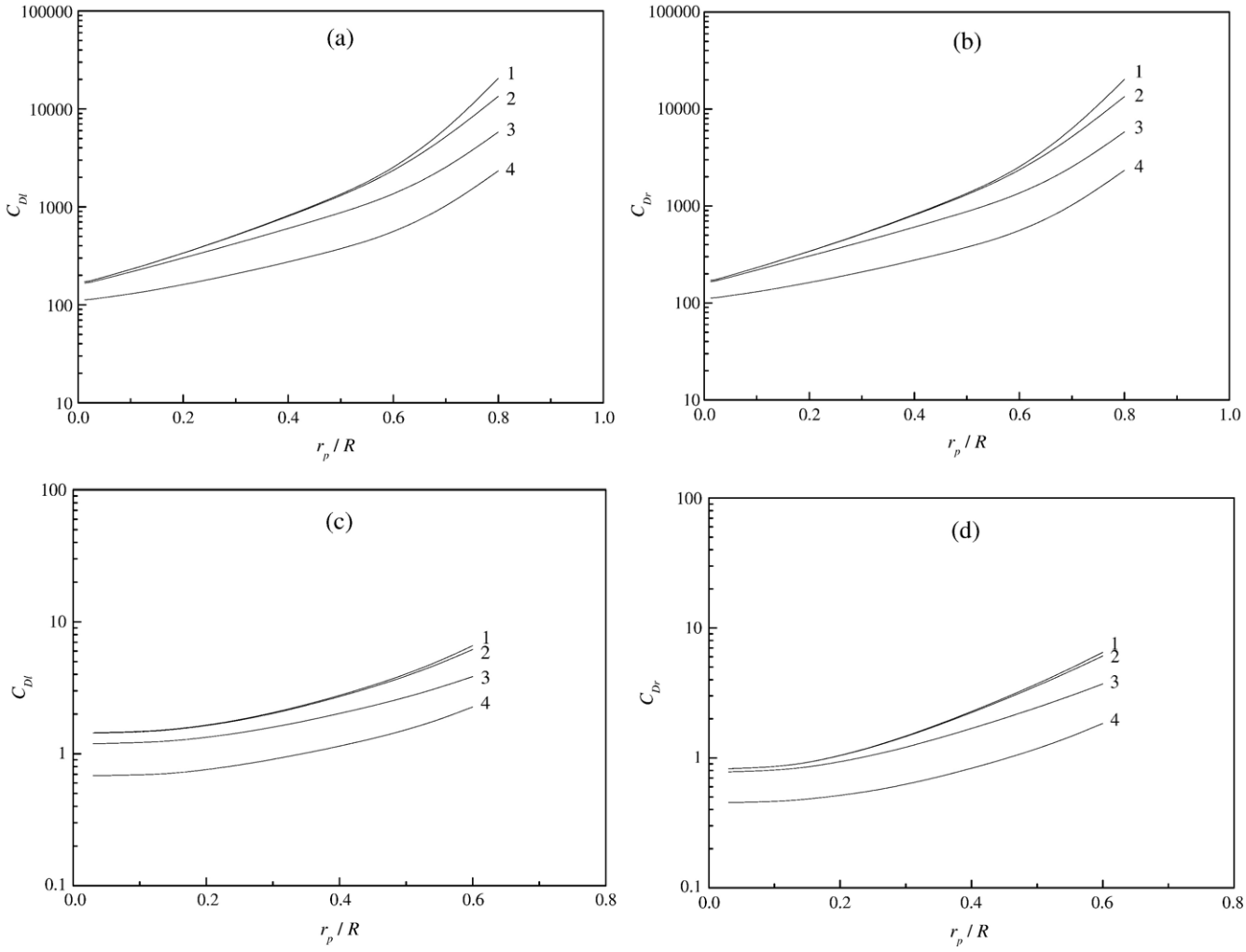

Fig. 8. Variations of C_{Dl}, (a) and (c), and C_{Dr}, (b) and (d), as a function of (r_p/R) for various combinations of Cu and Re at $S/d=2$ and $n=0.6$. Curve 1, $Cu=0$, 2, $Cu=0.1$, 3, $Cu=1$, 4, $Cu=10$. $Re=0.1$ in (a) and (b), and $Re=40$ in (c) and (d).

$(Cu=1)=0.95C_{Dr}(Cu=0))$, $(C_{Dl}(Cu=10)=0.48C_{Dl}(Cu=0))$, $(C_{Dr}(Cu=10)=0.56C_{Dr}(Cu=0))$. These imply that even if the boundary effect is absent, the shear-thinning nature of a fluid still plays an important role. As Re becomes larger, the inertial force acting on a sphere is more important than the corresponding viscous force. In this case, since the rear sphere is affected by the flow field behind the leading sphere the shear-thinning nature of the fluid near the rear sphere becomes less significant. For example, $(C_{Dl}(Cu=1)/C_{Dl}(Cu=0))<(C_{Dr}(Cu=1)/C_{Dr}(Cu=0))$ and $(C_{Dl}(Cu=10)/C_{Dl}(Cu=0)<C_{Dr}(Cu=10)/C_{Dr}(Cu=0))$. Also, $((C_D(Cu=1)/C_D(Cu=0)$ at $Re=40)<(C_D(Cu=1)/C_D(Cu=0))$ at $Re=0.1)$ and $((C_D(Cu=10)/C_D(Cu=0)$ at $Re=40)<(C_D(Cu=10)/C_D(Cu=0))$ at $Re=0.1)$. This is because the shear rate at $Re=40$ is sufficiently large to induce an appreciable decrease in the apparent viscosity of fluid. Fig. 9 illustrates the variations of C_{Dl} and C_{Dr} as a function of (r_p/R) for various combinations of n and Cu for the case when $S/d=2$ and Re is relatively small; that for the case when Re is relatively large is presented in Fig. 10. In Figs. 9a, b, 10a, and b, because Cu is small the influence of the shear-thinning nature of a fluid on the drag on a sphere is inappreciable. If $r_p/R<0.5$, the influence of n on C_D is inappreciable, even for $n=0.2$. Regardless of the value of Re, as Cu increases to unity, the influence of n on C_D becomes important, as can be seen in Figs. 9c, d, 10c, and d. For a fixed value of (r_p/R), C_D decreases with the decrease in n. This is because the smaller the value of n the more important the effect of shear thinning. In summary, the more significant the shear-thinning nature of a Carreau fluid the more appreciable its influence on C_D is. Figs. 11 and 12 show the variations of C_{Dl} and C_{Dr} as a function of (r_p/R) for various combinations of n and Cu at two levels of Re for the case when $S/d=10$. The qualitative behaviors of C_D are the same as that for the case when $S/d=2$.

Table 1 summarizes the boundary effect on the drag coefficients of two spheres, measured by $(C_D(r_p/R=0.6)/C_D(r_p/R=0))$; the larger this value the more important the effect. This table reveals that the general trend of the boundary effect

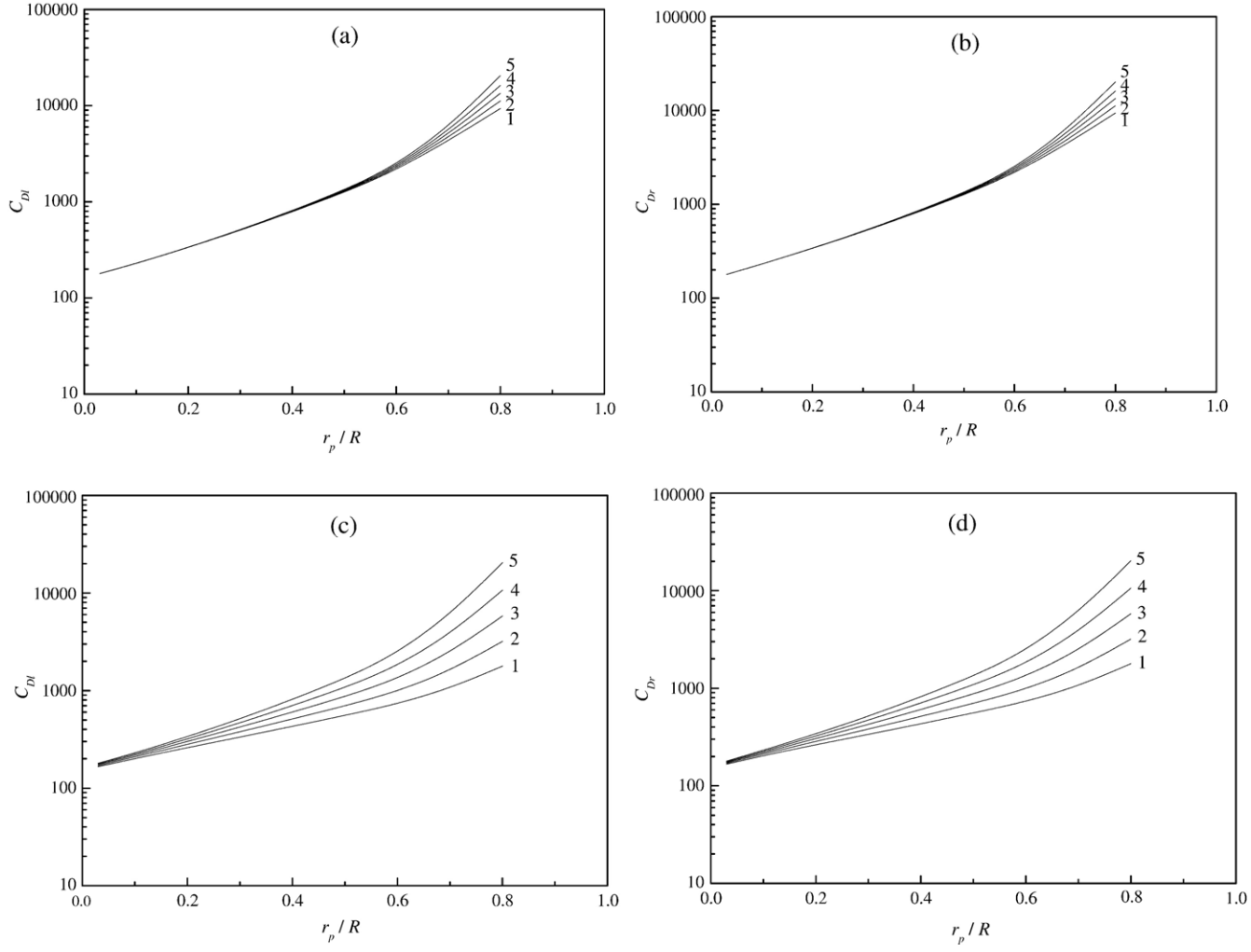

Fig. 9. Variations of C_{Dl}, (a) and (c), and C_{Dr}, (b) and (d), as a function of (r_p/R) for various combinations of n and Cu at $S/d=2$ and $Re=0.1$. Curve 1, $n=0.2$, 2, $n=0.4$, 3, $n=0.6$, 4, $n=0.8$, 5, $n=1$. $Cu=0.1$ in (a) and (b), and $Cu=1$ in (c) and (d).

on the leading sphere is the same as that on the rear sphere. For example, the boundary effect is less important if Re is large, (S/d) is large, n is small, and Cu is large. This result is similar to that observed by Hsu and Hsieh for the case of an isolated rigid particle in a cylinder filled with Carreau fluid [27]. If Re is small, the drag on the leading sphere is about the same as that on the rear sphere, and therefore, the degree of the boundary effect, measured by $(C_D(r_p/R=0.6)/C_D(r_p/R=0))$, of the leading sphere is about the same as that of the rear sphere. If Re is sufficiently large, regardless of the level of (S/d) and the property of fluid, the boundary effect on the leading sphere is always smaller than that on the rear sphere. This might arise from that if Re is large, the influence of the flow field behind the leading sphere on the rear sphere is significant, which enhances the boundary effect on the rear sphere. In general, if (S/d) is small, the influence of Re on the boundary effect on the rear sphere is more important than that when it is large. Therefore, the smaller the (S/d) is the larger the difference between the boundary effect on the leading sphere and that on the rear sphere.

3.3. Influence of Reynolds number

The variations of C_D as a function of Re for various values of Cu and (r_p/R) at two levels of (S/d) are illustrated in Figs. 13 and 14. According to Eq. (11), $\ln(C_D)$ and $\ln(Re)$ are linearly correlated for the case of Newtonian fluid in the creeping flow regime. If the Stokes'-law-like relation expressed in Eq. (12) exists, then a plot of $\ln(C_D)$ against $\ln(Re)$ should give a straight line. Regardless of the level of (S/d), the deviation of C_D from the Stokes'-law-like relation depends upon the magnitude of (r_p/R); the smaller the (r_p/R) the more serious is the deviation. Table 2 summarizes the percentage deviations of C_D from a Stokes'-law-like relation at $Re=40$ for various combinations of (r_p/R) and (S/d). The percentage deviation of C_D is defined by $[(C_D-C_D')/C_D']\times 100\%$, where C_D' is the drag coefficient based on the Stokes'-law-like relation. Regardless of the level of (S/d), the shear-thinning nature of a fluid has the effect of reducing the percentage deviation of C_D from the Stokes'-law-like relation when the boundary effect is insignificant $(r_p/R=0.1)$. If the boundary effect is significant $(r_p/R=0.6)$, the percentage

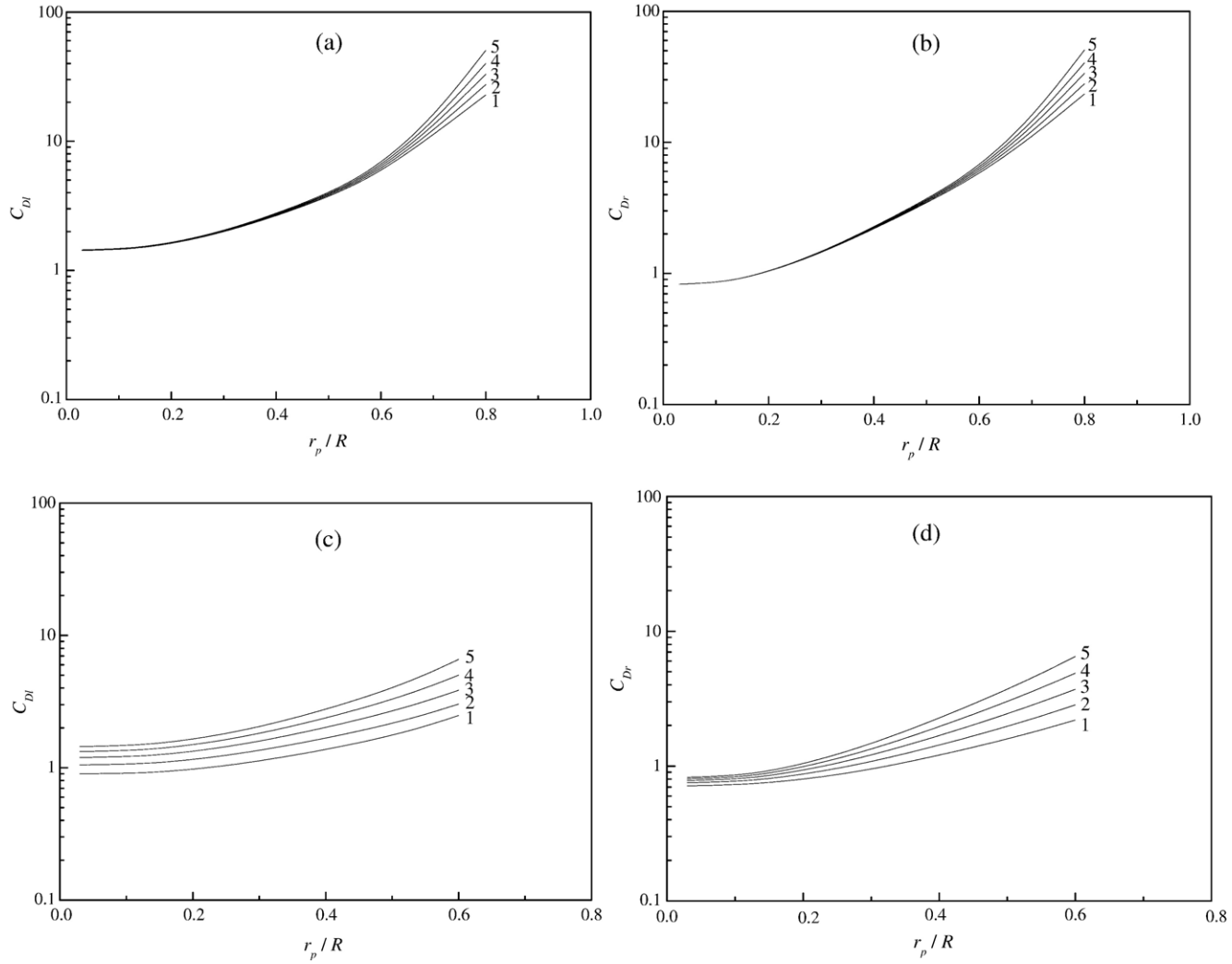

Fig. 10. Variations of C_{Dl}, (a) and (c), and C_{Dr}, (b) and (d), as a function of (r_p/R) for various combinations of n and Cu at $S/d=2$ and $Re=40$. Curve 1, $n=0.2$, 2, $n=0.4$, 3, $n=0.6$, 4, $n=0.8$, 5, $n=1$. $Cu=0.1$ in (a) and (b), and $Cu=1$ in (c) and (d).

deviation of C_D has a local minimum as Cu varies. For $r_p/R=0.6$ and $n=0.6$, the value of Cu at which the local minimum occurs is in the range $0.1 \le Cu < 1$. The occurrence of the local minimum might arise from that when boundary effect is important, the wall-sphere distance is sufficiently small and the flow field between them is compressed. In this case, the shear-thinning nature of a fluid is enhanced, and the deviation of C_D from the Stokes'-law-like relation increases accordingly. The above reasoning also implies that when the properties of a fluid are fixed the deviation of C_D may have a local minimum as (r_p/R) varies. For the case when $Cu=1$ and $n=0.6$, if $S/d=2$, the deviations of C_D from the Stokes'-law-like relation of the rear sphere for $r_p/R=0.1$, 0.3, 0.5, and 0.6 are 46.40, 10.41, 11.47, and 12.46%, respectively, and the corresponding deviations of C_D of the leading sphere are 124.29, 46.99, 21.54, and 16.63%. If $S/d=10$, the deviations of C_D of the rear sphere for $r_p/R=0.1$, 0.3, 0.5, 0.6, and 0.7 are 83.67, 41.63, 23.38, 12.29, and 25.33%, respectively, and the corresponding deviations of the leading sphere are 107.77, 43.59, 19.11, 10.37, and 0.57%. Because the rear sphere is not only affected by the cylinder wall but also by the flow field behind the leading sphere, the deviation of C_D of the rear sphere is more likely to have a local minimum as (r_p/R) varies for the case when $Cu=1$ and $n=0.6$ than that of the leading sphere. Note that the smaller the (S/d) the easier to observe a local minimum. As can be seen in Table 2, the deviation of C_D of the rear sphere at $S/d=2$ is smaller than that at $S/d=10$; but the reverse is true for the leading sphere. This might due to that if (S/d) is small, the rear sphere is affected significantly by the flow field behind the leading sphere. If (S/d) is small, the deviation of C_D of the rear sphere from the Stokes'-law-like relation is much smaller than that of the leading sphere. Table 2 also shows that if $S/d=2$, the deviation of C_D of the rear sphere is always smaller than that of the leading sphere. If $S/d=10$, the deviation of C_D of the rear sphere is smaller than that of the leading sphere when the boundary effect is insignificant $(r_p/R=0.1)$, but the reverse is true if it is significant

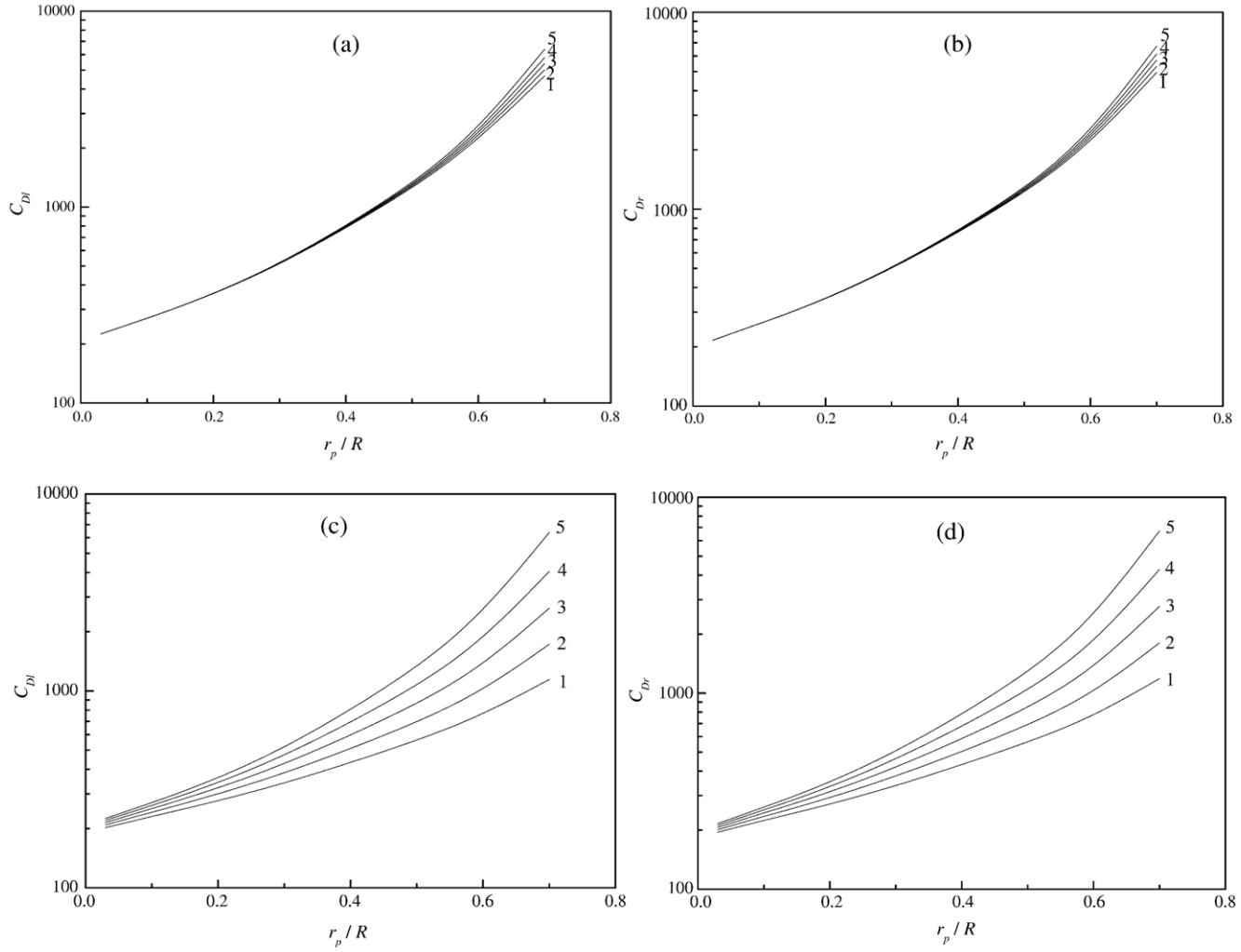

Fig. 11. Variations of C_{Dl}, (a) and (c), and C_{Dr}, (b) and (d), as a function of (r_p/R) for various combinations of n and Cu at $S/d=10$ and $Re=0.1$. Curve 1, $n=0.2$, 2, $n=0.4$, 3, $n=0.6$, 4, $n=0.8$, 5, $n=1$. $Cu=0.1$ in (a) and (b), and $Cu=1$ in (c) and (d).

$(r_p/R=0.6)$. In fact, the deviation of C_D from the Stokes'-law-like relation is not only affected by the interaction between two spheres but also by the boundary effect. If the latter is insignificant, then the deviation is dominated by the former, and therefore, regardless of the value of (S/d), the deviation of the rear sphere is smaller than that of the leading sphere. On the other hand, if the boundary effect is significant, the relative levels of the deviations of C_D for the leading and the rear spheres still depends upon (S/d). For example, if $S/d=2$ (boundary effect < interaction between two spheres), the deviation of C_D of the rear sphere is smaller than that of the leading sphere. However, if $S/d=10$ (boundary effect > interaction between two spheres), the deviation of C_D of the rear sphere is slightly larger than that of the leading sphere. Also, if the boundary effect is important, regardless of the level of (S/d), the deviation of C_D for both spheres increases with the increase in Cu.

3.4. Critical center-to-center distance

Table 3 summarizes the critical center-to-center distances (S_c/d) at various combinations of (r_p/R), Re, and Cu for the case when $n=0.8$, where (S_c/d) is defined as the value of (S/d) when $(C_{Dr}/C_{D\infty})\cong 97\%$, $C_{D\infty}$ being the drag coefficient of an isolated sphere. If $(S/d)>(S_c/d)$, the interaction between two particles is negligible, that is, they can be treated as isolated particles. No general trend is observed for the behavior of (S_c/d) at $Cu=1$ and 10. However, (S_c/d) declines with the increase of (r_p/R). That is, the existence of the cylinder has the effect of reducing the interaction between two particles. As Re increases, the interaction between two spheres becomes more important, and the critical center-to-center distance (S_c/d) becomes larger accordingly.

A comparison of the results obtained in this study with those of Hsu et al. [27] reveals that for both Newtonian and Carreau fluids the influences of the wall and the nature of a fluid on C_D for two spheres are similar to those for a single sphere. However, the behavior of the percentage deviation of C_D from a Stokes'-law-like relation at $Re=40$ for these two cases can be different. The percentage deviation for the case of two spheres is always smaller than that for the case of a single sphere. That is, the presence of a nearby sphere has the effect of reducing that percentage deviation. Also, the closer the spheres the larger

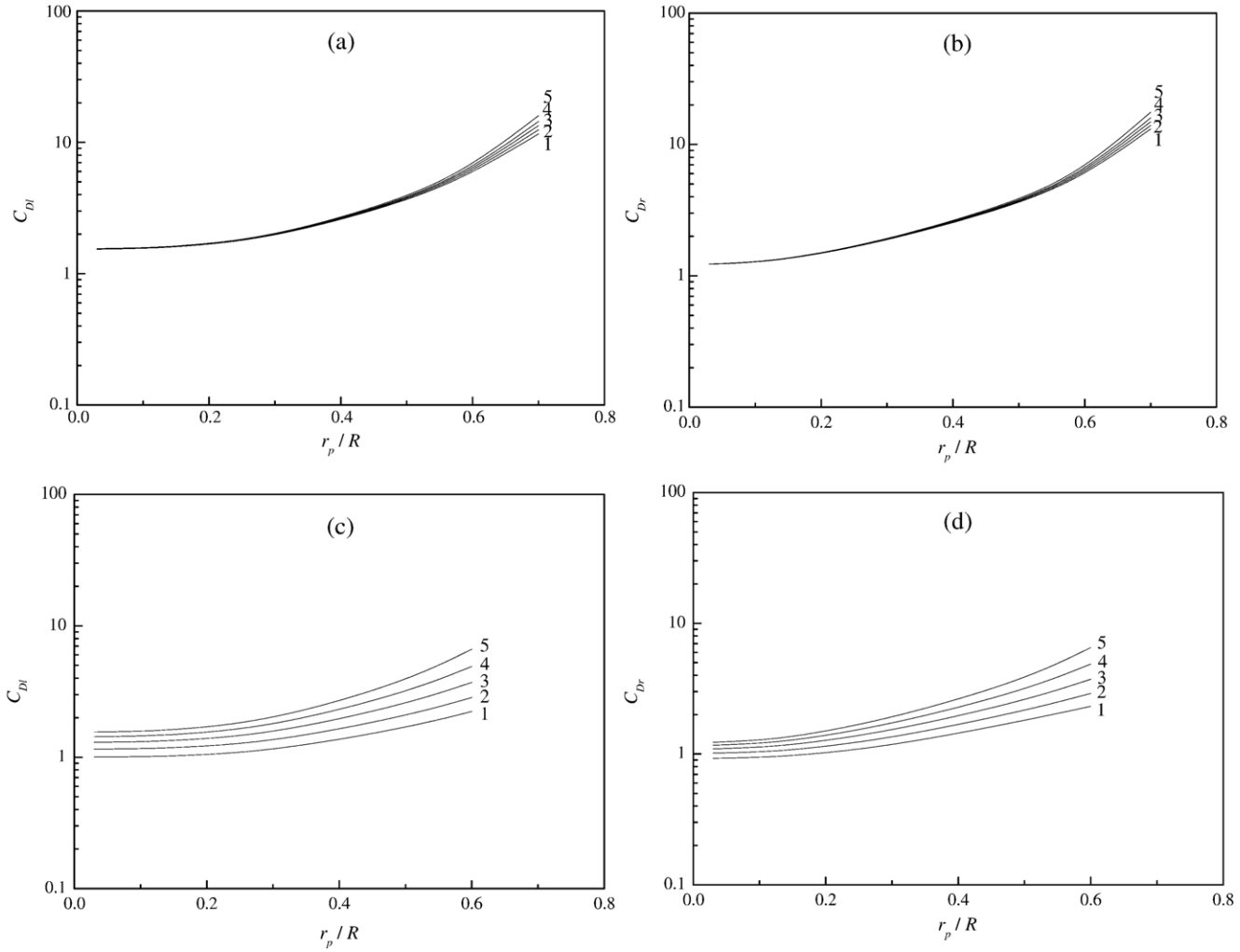

Fig. 12. Variations of C_{Dl}, (a) and (c), and C_{Dr}, (b) and (d), as a function of (r_p/R) for various combinations of n and Cu at $S/d=10$ and $Re=40$. Curve 1, $n=0.2$, 2, $n=0.4$, 3, $n=0.6$, 4, $n=0.8$, 5, $n=1$. $Cu=0.1$ in (a) and (b), and $Cu=1$ in (c) and (d).

the reduction in the percentage deviation, and the reduction of the rear sphere is larger than that of the leading sphere. If the boundary effect is relatively unimportant, the general behavior of the percentage deviation for the case of two spheres is the same as that of a single sphere. On the other hand, if the boundary effect is important, the percentage deviation increases monotonically with the increase in Cu for the case of a single sphere, but it has a local minimum as Cu varies for the case of two spheres. The latter implies that the wall effect and the influence of fluid nature on the behavior of sphere become more complicated when a nearby sphere is present.

4. Conclusion

The presence of a boundary and neighboring particles and the non-Newtonian nature of a fluid on the drag on a particle are investigated by considering the translation of two identical, rigid spheres along the axis of a long cylinder filled with a Carreau fluid. We consider the case when Reynolds number is in the range (0.1, 40), Carreau number in the range (0, 10), power law index in the range (0.2, 1), the ratio (radius of sphere/radius of cylinder) in the range (0, 0.8), and the ratio (center-to-center distance/diameter of particle) in the range (1, 20). The results of numerical calculations can be summarized as following. (a) For a medium large Reynolds number if the boundary effect is important, the convective motion of a fluid, which has the effect to have the flow field reversed, is enhanced by its shear-thinning nature. (b) The more important the shear-thinning nature of a fluid and/or the larger the Reynolds number, the smaller the critical radius of a cylinder, the radius beyond which the boundary effect becomes negligible. (c) The smaller the Reynolds number and/or the separation distance between two spheres the more significant the boundary effect. In this case the shear-thinning nature of a fluid becomes inappreciable. (d) The shear-thinning nature of a fluid has the effect of reducing the deviation of the ln(drag coefficient)-ln(Reynolds number) curve from a Stokes'-law-like relation when the boundary effect is insignificant. On the other hand, if it is significant, the deviation has a local minimum as the shear-thinning nature of a fluid varies. (e) The presence of the cylinder

Table 1
Influence of boundary on the drag on a sphere for various combinations of (S/d), Re, Cu, and n

S/d	Re	Cu	n	$C_D(r_p/R=0.6)/C_D(r_p/R=0)$	
				Leading sphere	Rear sphere
2	0.1	0.1	0.2	12.43	12.53
			0.4	12.82	12.93
			0.6	13.21	13.33
			0.8	13.61	13.72
			1	14.03	14.15
		1	0.2	4.53	4.52
			0.4	5.96	5.96
			0.6	7.89	7.92
			0.8	10.50	10.56
			1	14.03	14.15
		10	0.2	2.10	2.09
			0.4	3.05	3.04
			0.6	4.80	4.78
			0.8	8.01	8.03
			1	14.03	14.15
10	0.1	0.1	0.2	10.20	10.61
			0.4	10.51	10.91
			0.6	10.83	11.21
			0.8	11.16	11.51
			1	11.61	11.95
		1	0.2	3.87	4.07
			0.4	4.99	5.22
			0.6	6.52	6.79
			0.8	8.62	8.93
			1	11.61	11.95
		10	0.2	1.83	1.87
			0.4	2.65	2.72
			0.6	4.08	4.20
			0.8	6.68	6.89
			1	11.61	11.95
2	40	0.1	0.2	3.95	6.59
			0.4	4.07	6.81
			0.6	4.18	7.03
			0.8	4.30	7.25
			1	4.43	7.50
		1	0.2	2.68	2.90
			0.4	2.80	3.59
			0.6	3.13	4.52
			0.8	3.67	5.78
			1	4.43	7.50
10	40	0.1	0.2	3.68	4.52
			0.4	3.78	4.63
			0.6	3.89	4.75
			0.8	3.99	4.88
			1	4.16	5.07
		1	0.2	2.16	2.38
			0.4	2.39	2.73
			0.6	2.77	3.25
			0.8	3.33	3.99
			1	4.16	5.07

has the effect of reducing the interaction between two spheres. However, the larger the Reynolds number the more important is the interaction between two spheres.

Acknowledgment

This work is supported by the National Science Council of the Republic of China.

References

[1] R.P. Chhabra, Powder Technol. 85 (1995) 83.
[2] R.P. Chhabra, S. Agarwal, K. Chaudhary, Powder Technol. 129 (2003) 53.
[3] M. Stimson, G.B. Jeffery, Proc. R. Soc. Lond., A 111 (1926) 110.
[4] J. Happel, R. Pfeffer, Am. Inst. Chem. Eng. J. 6 (1960) 129.
[5] C. Zhu, S.C. Liang, L.S. Fan, Int. J. Multiph. Flow 20 (1994) 117.
[6] S.C. Liang, T. Hong, L.S. Fan, Int. J. Multiph. Flow 22 (1996) 285.
[7] R.C. Chen, Y.N. Lu, Int. J. Multiph. Flow 25 (1999) 1645.
[8] R.C. Chen, J.L. Wu, Chem. Eng. Sci. 55 (2000) 1143.
[9] T. Greenstein, J. Mech. Eng. Sci. 22 (1980) 243.
[10] A. Maheshwari, R.P. Chhabra, G. Biswas, Powder Technol. 168 (2006) 74.
[11] S.M. Barnett, A.E. Humphrey, M. Litt, Am. Inst. Chem. Eng. J. 12 (1966) 253.
[12] E. Zana, L.G. Leal, Int. J. Multiph. Flow 4 (1978) 237.
[13] R.P. Chhabra, D. DeKee, Fluid Particles in Rheologically Complex Media, Transport Processes, Bubbles, Drops and Particles, Hemisphere, New York, 1992.
[14] R.P. Chhabra, Bubbles, Drops and Particles in Non-Newtonian Fluids, CRC Taylor & Francis, 2007.
[15] M.J. Riddle, C. Narvaez, R.B. Bird, J. Non-Newton. Fluid Mech. 2 (1977) 23.
[16] R.P. Chhabra, C. Tiu, P.H.T. Uhlherr, Can. J. Chem. Eng. 59 (1981) 771.
[17] P.Y. Huang, J. Feng, D.D. Joseph, J. Fluid Mech. 271 (1994) 1.
[18] A. Tripathi, R.P. Chhabra, T. Sundararajan, Ind. Eng. Chem. Res. 33 (1994) 403.
[19] R.P. Chhabra, P.H.T. Uhlherr, Can. J. Chem. Eng. 58 (1980) 124.
[20] Y.J. Liu, D.D. Joseph, J. Fluid Mech. 255 (1993) 255.
[21] K.A. Missirlis, D. Assimacopoulos, E. Mitsoulis, R.P. Chhabra, J. Non-Newton. Fluid Mech. 96 (2001) 459.
[22] K. Ceylan, S. Herdem, T. Abbasov, Powder Technol. 103 (1999) 286.
[23] I. Machač, B. Šiška, L. Machačcvá, Chem. Eng. Process. 39 (2000) 365.
[24] I. Machač, B. Šiška, R. Teichman, Chem. Eng. Process. 41 (2002) 577.
[25] A.K. Jaiswal, T. Sundararajan, R.P. Chhabra, Int. J. Eng. Sci. 31 (1993) 293.
[26] C. Zhu, K. Lam, H.H. Chu, X.D. Tang, G. Liu, Mech. Res. Commun. 30 (2003) 651.
[27] J.P. Hsu, Y.H. Hsieh, S. Tseng, J. Colloid Interface Sci. 284 (2005) 729.
[28] S. Daugan, L. Talini, B. Herzhaft, C. Allain, Eur. Phys. J., E Soft Matter 7 (2002) 73.
[29] S. Daugan, L. Talini, B. Herzhaft, C. Allain, Eur. Phys. J., E Soft Matter 9 (2002) 55.
[30] W.B. Huang, H.Y. Li, Y. Xu, G.P. Lian, Mech. Eng. Sci. 61 (2006) 1480.
[31] R.B. Bird, R.C. Armstrong, O. Hassager, Dynamics of Polymeric Liquids, Wiley, New York, 1977.
[32] H.A. Barnes, J.F. Hutton, K. Walters, An Introduction to Rheology, Elsevier, New York, 1989.
[33] J. Ferguson, Z. Kemblowski, Applied Fluid Rheology, Elsevier, New York, 1991.
[34] R. Clift, J. Grace, M.E. Weber, Bubbles, Drops and Particles, Academic Press, 1978.
[35] R.M. Turian, Am. Inst. Chem. Eng. J. 13 (1967) 999.
[36] R.B. Bird, W.E. Stewart, E.N. Lightfoot, Transport Phenomena, John Wiley and Sons, New York, 2002.
[37] G. McKinley, Transport Processes in Bubbles, Drops and Particles, 2nd ed. Taylor & Francis, New York, 2002.

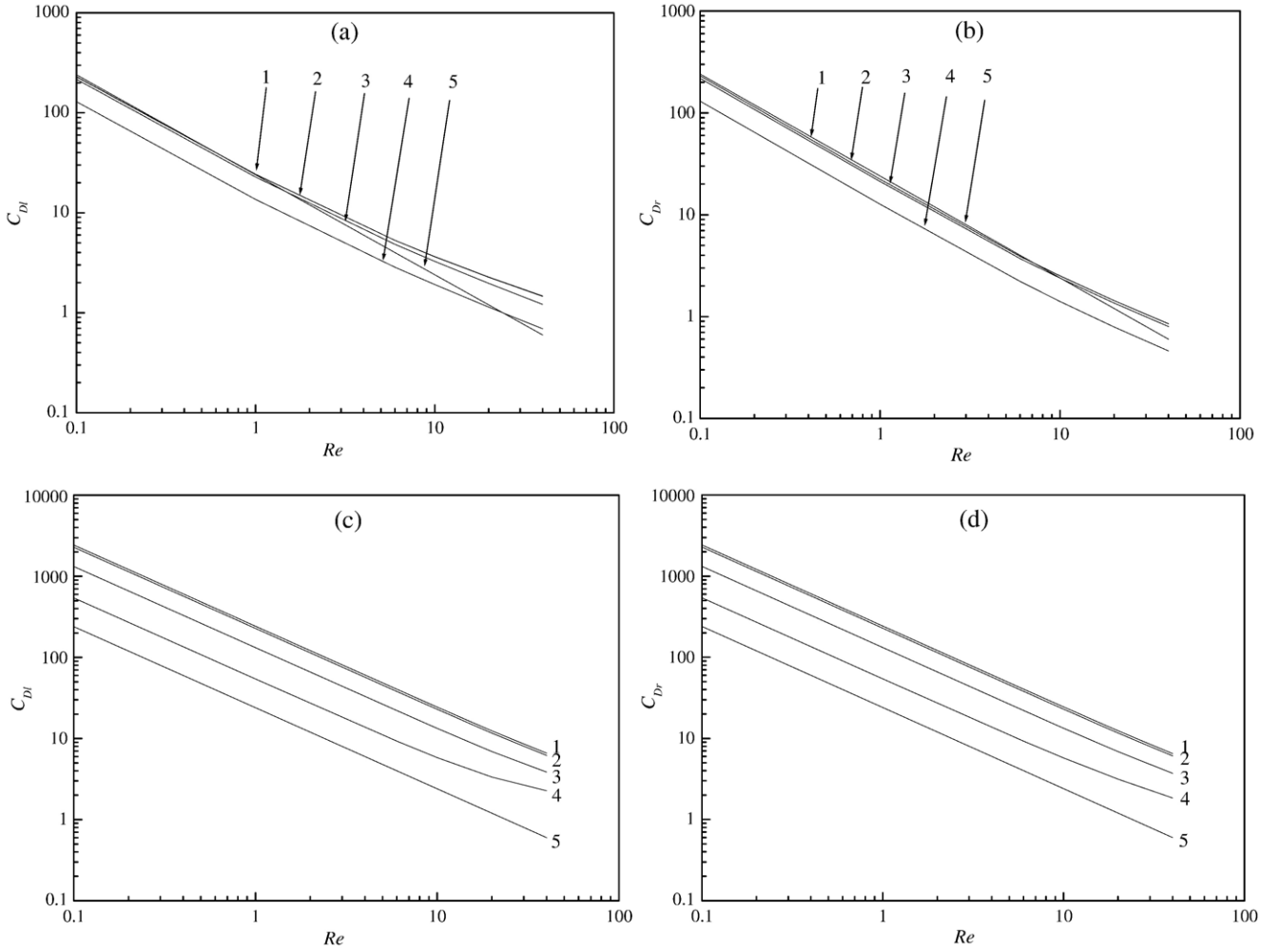

Fig. 13. Variations of C_{Dl}, (a) and (c), and C_{Dr}, (b) and (d), as a function of Re for various combinations of Cu and (r_p/R) for the case when $S/d=2$ and $n=0.6$. Curve 1, $Cu=0$, 2, $Cu=0.1$, 3, $Cu=1$, 4, $Cu=10$, 5, Stokes' law. $r_p/R=0.1$ in (a) and (b), and $r_p/R=0.6$ in (c) and (d).

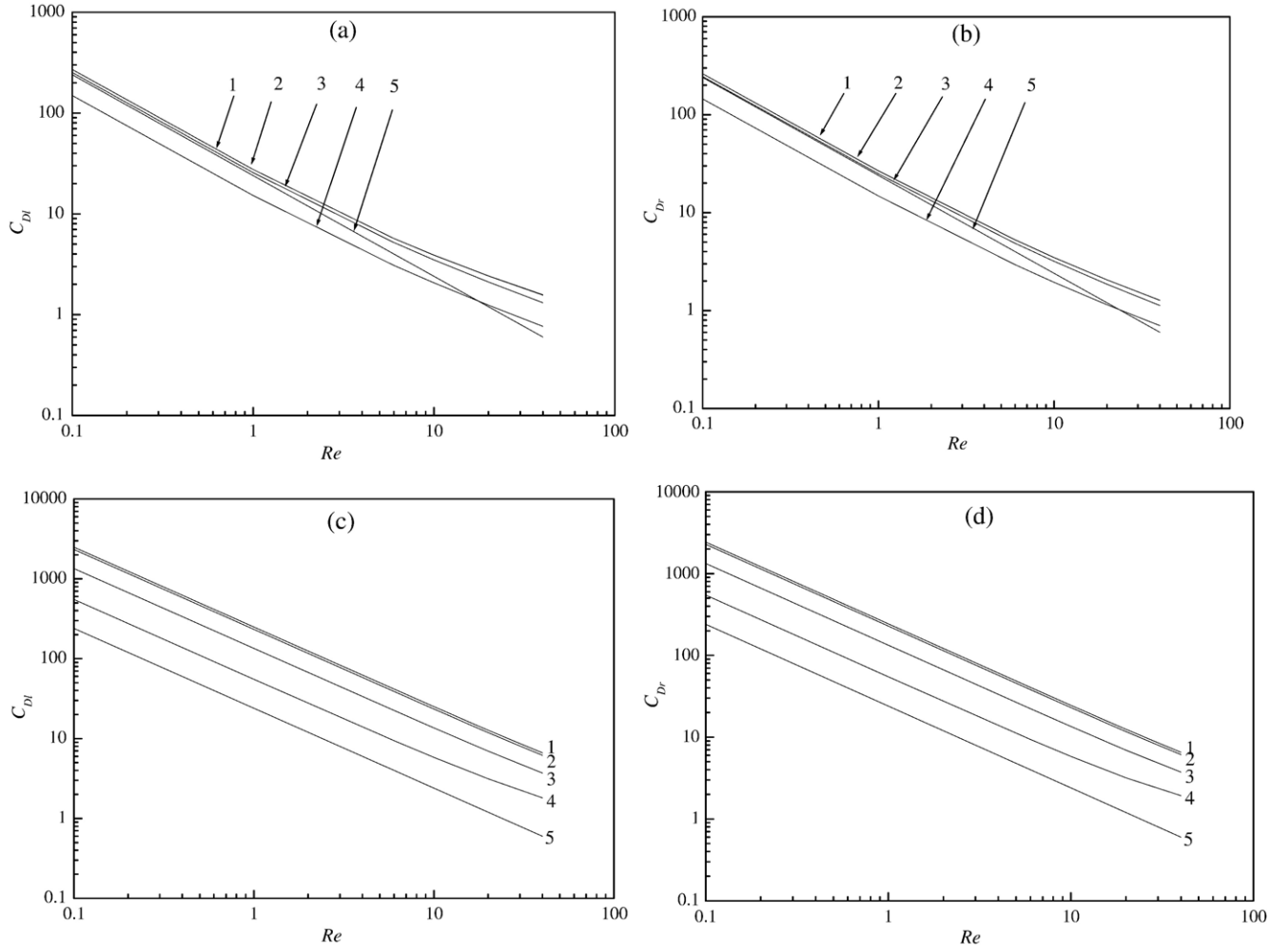

Fig. 14. Variations of C_{Dl}, (a) and (c), and C_{Dr}, (b) and (d), as a function of Re for various combinations of Cu and (r_p/R) for the case when $S/d=10$ and $n=0.6$. Curve 1, $Cu=0$, 2, $Cu=0.1$, 3, $Cu=1$, 4, $Cu=10$, 5, Stokes' law. $r_p/R=0.1$ in and (b), and $r_p/R=0.6$ in (c) and (d).

Table 2
Percentage deviation of C_D from a Stokes'-law-like relation at $Re=40$ and $n=0.6$ for various combinations of (S/d), (r_p/R), and Cu

S/d	r_p/R	Cu	Percentage deviation (%)	
			Leading sphere	Rear sphere
2	0.1	0	156.35	47.08
		0.1	154.98	47.18
		1	124.29	46.40
		10	114.14	41.39
	0.6	0	8.56	7.00
		0.1	8.27	6.67
		1	16.63	12.46
		10	66.94	36.19
10	0.1	0	132.55	94.13
		0.1	131.42	93.70
		1	107.77	83.67
		10	104.85	93.60
	0.6	0	6.44	7.47
		0.1	6.00	7.14
		1	10.37	12.29
		10	31.46	40.97

Table 3
Critical center-to-center distance (S_c/d) at $n=0.8$ for various combinations of Re, Cu, and (r_p/R)

Re	Cu	r_p/R	S_c/d
0.1	1	0	12.49
		0.1	4.87
		0.3	1.93
		0.5	1.28
	10	0	12.08
		0.1	4.74
		0.3	2.08
		0.5	1.45
10	1	0	14.91
		0.1	13.25
		0.3	6.16
		0.5	1.82
	10	0	14.49
		0.1	13.08
		0.3	4.92
		0.5	1.94
40	1	0	18.97
		0.1	18.17
		0.3	14.03
		0.5	14.19
	10	0	20.10
		0.1	19.46
		0.3	13.11
		0.5	12.80